Density Functional Theory Studies of Thermal Activation of Methane by MH^+ (M = Ru, Rh, and Pd)

Wenqiang Li, Zhiyuan Geng,* Yongcheng Wang, PenJi Yan, Xu Zhang, Zheng Wang, and Fengxia Liu

Gansu Key Laboratory of Polymer Materials, College of Chemistry and Chemical Engineering Northwest Normal University, Lanzhou 730070, People's Republic of China

Received: May 12, 2008; Revised Manuscript Received: December 6, 2008

The dehydrogenation reaction mechanisms of methane catalyzed by a ligated transition metal MH^+ (M = Ru, Rh, and Pd) have been investigated theoretically. Activation of methane by MH^+ complexes is proposed to proceed in a one-step manner via one transition state: $MH^+ + CH_4 \rightarrow MH^+CH_4 \rightarrow [TS] \rightarrow (MCH_3^+)H_2 \rightarrow MCH_3^+ + H_2$. Both high-spin and low-spin potential energy surfaces are characterized in detail. Our calculations indicate that the ground-states species have low electron spin and a dominant $4d^n$ configuration for RuH^+, RhH^+, and PdH^+, and the whole reaction proceeds on the ground-states potential energy surfaces with a spin-allowed manner. The MH^+ (M = Ru, Rh, and Pd) complexes are expected from the general energy profiles of the reaction pathways to efficiently convert methane to metal methyl, thus RuH^+, RhH^+, and PdH^+ are likely to be excellent mediators for the activity of methane. In the reactions of MH^+ with methane, the H_2 elimination from the dihydrogen complex is quite facile without barriers. The exothermicities of the reactions are close for Ru, Rh, and Pd: 11.1, 1.2, and 5.2 kcal/mol, respectively.

I. Introduction

The activation of C−H and C−C bonds of alkanes by gas-phase atomic transition metal ions has been studied intensely over the past decade because of its immense scientific and industrial importance.[1−5] In particular, the cleavage of the C−H bond in methane is an industrial process of great interest because it is the first step in converting natural gas into a transportable liquid feedstock. A number of experimental and theoretical studies of atomic transition metal ions with small alkanes have provided a wealth of insight concerning the intrinsic interactions of metal ions with bonds composed of carbon and hydrogen atoms.[6−15] The studies demonstrate that methane can be spontaneously activated by the third-row transition metal ions Os^+, Ir^+, Pt^+, etc., yielding the metallic carbene cations and H_2. Second-row transition metal cations are found to be much less reactive toward methane than their third row counterparts, and activation of methane is rarely observed. Equilibrium and DFT studies performed on first-row transition metal ions (Cr, V, Fe, Co, and Ni) showed that methane molecules sequentially cluster to the ionic metal centers leaving the C−H bonds intact.[16]

An alternative approach to probe the activation of the C−H bond in methane is to start with ligated transition metal ions.[17,18] The immediate effects of the ligands are to alter the electronic structure of the metal center through selective tuning of the electronic states. The addition of a single ligand to the metal center can dramatically alter the reactivity.[19−23] For example, Mn^+ is the least reactive 3d transition metal cation toward alkanes, whereas $[MnO]^+$ is the most reactive one.[24,25] An extraordinary ligand effect has been also reported for diatomic $[MH]^+$ ions (M = Fe, Co, and Ni); whereas the naked metal ions M^+ do not bring about thermal C−H bond cleavage, $[NiH]^+$ activates methane at temperatures as low as 80 K, $[CoH]^+$ reacts at room temperature, and for $[FeH]^+$ temperatures above 600 K are required for the H/CH_3 ligand exchange, which is exothermic for all three metal hydrides.[26]

Very recently, an experimental and theoretical investigation of methane dehydrogenation by PdH^+ in the gas phase has been reported by Schlangen and Schwarz.[27] The results have shown that the PdH^+ can effectively activate the C−H bond in methane. There is no experimental and theoretical study about the second-row transition metal ions ligated by hydrogen so far as we know, though this kind of reactions is very significant. In this paper, we have systematically carried out a theoretical investigation at the DFT level of the activation of the C−H bond in methane by MH^+ for M = Ru, Rh, and Pd, which are expected to provide some helpful information to experimentalists who are interested in this area. Our study intends to resolve the four following problems: (i) What are the mechanistic details of methane catalyzed by ligated transition metal MH^+ (M = Ru, Rh, and Pd)? (ii) How do the ligands affect the reactions: (iii) as compared with their first-row congeners, whether they have the same reactive character; (iv) as compared with M^+ (M = Ru, Rh, and Pd), whether MH^+ (M = Ru, Rh, and Pd) can better activate C−H bond in methane.

II. Method of Calculation

The detailed quantum chemical studies on the mechanism of the methane catalyzed by ligated transition metal MH^+ (M = Ru, Rh, and Pd) are reported in this paper. The stationary structures of the potential energy surfaces were fully optimized at the B3LYP level of theory.[28−30] Analytical frequency calculations at the same level of theory were performed in order to confirm the optimized structures to either a minimum or a first-order saddle point as well as to obtain the zero-point energy correction. Furthermore, intrinsic reaction coordinate (IRC) calculations[31] were performed to confirm that the optimized transition states correctly connect the relevant reactants and products. Geometry optimization for all of the reactants, intermediates, transition states, and products as well as the frequency calculations were carried out with the 6-31+G** basis set for the carbon, hydrogen atoms of the reactions investi-

10.1021/jp808830c CCC: $40.75
Published on Web 02/06/2009

SCHEME 1

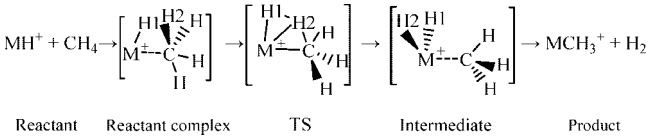

gated.[32] Also, the relativistic core potentials (RECP)[33] of Stuttgart were used for Ru, Rh, and Pd atom, and the 4d and 5s in Ru, Rh, and Pd are treated explicitly by a (8s7p6d) Gaussian basis set contracted to [6s5p3d].[34,35] All calculations used the RECP in which 4s, 4p, 4d, and 5s electrons were explicitly treated as "valence" electrons with the remaining electrons replaced by the RECP. Thus, 16, 17, and 18 valence electrons RECP were used for the Ru, Rh, and Pd centers, respectively. All of calculations were performed with the Gaussian 98 program.[36]

III. Results and Discussion

The concerted reaction pathway for activation of methane by MH^+ (M = Ru, Rh, and Pd) complexes via one transition state of direct dehydrogenation has been studied, as indicated in Scheme 1. To better understand of the reaction, the electronic structures of the reactants (MH^+) and products (MCH_3^+) have been analyzed and the features of transition states (TS) have been discussed. Also some comparisons with the similar reactions have been performed for achieving more reasonable information.

A. Electronic Structures of the MH^+ and MCH_3^+ (M = Ru, Rh, and Pd). Let us begin by looking at the general electronic features of the MH^+ complexes and the reliability of the energetics computed with a combination of the B3LYP method and the basis sets mentioned above. Schilling et al. have predicted the bonding characters of the MH^+ and MCH_3^+ complexes from generalized valence bond calculations.[37] The metal−hydrogen bond is significantly dependent on the character of d orbitals. In the first transition row the 4s orbital is much larger than 3d, making the 4s more available for the bond to H. In the second row, the 5s and 4d orbitals are more similar in size, leading to much larger d character in the bond orbitals.

For RuH^+, the ground electronic state is $^3\Sigma O^-$, which is mainly derived from the $4d^7$ (^4F) state of atomic Ru^+. The 1s orbital of H and d_{z^2} orbital of Ru^+ form σ covalent bond, and each of the d_{xy} and $d_{x^2-y^2}$ orbitals of Ru^+ has one unpaired electron. For RhH^+, the best d^8 (^3F) configuration has singly occupied d_{z^2} and $d\delta$ orbitals leading to $^2\Delta$ states. For Pd^+ with a d^9 configuration a singly occupied d_{z^2} orbital combined with a 1s orbital of H leads to a $^1\Sigma^+$ state for PdH^+. The quartet state of RuH^+ and triplet state of PdH^+ are expected to be much higher in energy due to the large d^n to s^1d^{n-1} promotion energies. As there is no loss of exchange energy in forming the PdH^+ bond, the bond dissociation energies (BDE) is relatively strong. The computed bond lengths and BDE of the ground states and excite states for the MH^+ complexes are shown in Table 1, the BDE of PdH^+ is 49.1 kcal/mol, whereas RuH^+ and RhH^+ are 36.8 and 44.3 kcal/mol respectively, which are qualitatively consistent with the experimental values. (the experimental value of the BDE of RuH^+, RhH^+, and PdH^+ are 41, 42, and 45 kcal/mol, respectively).[38]

For the electronic features of the MCH_3^+ complexes, the bond between a transition metal and the methyl radical can be visualized as spin pairing of an electron in a metal σ orbital (a hybrid containing s, d_{z^2}, and p_z character) with the unpaired electron of CH_3 (in a carbon hybrid orbital containing s and p_z character). The interaction of the metal nonbonding electrons in the metal methyls is found to be very similar to that of the metal hydride ions, so we consider the electric state is corresponding to the ground state of MH^+.

TABLE 1: Computed Bond Distances, Vibrational Frequencies, and BDEs for the MH^+ Complexes and the Experimental Data

species	state	r(M−H) (Å)	vibrational frequency (cm^{-1})	BDE[a]
RuH^+	3	1.518	2154.0	36.8(41)
	5	1.640	1767.0	23.0
RhH^+	2	1.501	2266.0	44.3(42)
	4	1.558	2049.0	25.9
PdH^+	1	1.474	2315.0	49.1(45)
	3	1.580	1805.0	29.6

[a] The BDE in parentheses are the experimental values.

B. Multicenter Transition State (MCTS). Structures of the MCTSs that were determined by DFT calculations are displayed in Figure 1 for Ru, Rh, and Pd systems (the detailed information of reactants, intermediates, and products were displayed in Supporting Information). The transition vectors leading to the C−H bond cleavage and the corresponding imaginary frequencies are shown as well. A four-membered ring, composed of the MH^+ reactant and a C−H pair from methane, exists for both the low-spin and high-spin M^+HHCH_3 transition states. One of the hydrogen atoms from methane shifts to the metal via the four-membered MCTSs, giving rise to the $MCH_3^+(H_2)$ molecular complex. The NBO valence electron populations of the low-spin and high-spin MCTSs are calculated to be $4d^{7.23}5s^{0.11}/4d^{6.73}5s^{0.34}$, $4d^{8.14}5s^{0.32}/4d^{7.71}5s^{0.39}$, and $4d^{9.27}5s^{0.15}/4d^{8.86}5s^{0.38}$ for M = Ru, Rh, and Pd, respectively. The low-spin transition states, which have less 5s electronic density on the metal centers, have more compact structures than their high-spin analogues. For the low-spin Ru^+HHCH_3 MCTSs shown in Figure 1a, the activated C−H bond is elongated to 1.52 Å compared to a calculated C−H distance of 1.09 Å in an isolated methane molecule. The H−H distance is 1.05 Å, which is 0.27 Å longer than the normal H−H bond. The Rh and Pd MCTS structures as shown in parts b and c of Figure 1 are comparable to that of the Ru structure.

C. Reactivity of MH^+ (M = Ru, Rh, and Pd) toward Methane. Figure 2 presents the relative energy profiles of reactions of MH^+ with methane. Corresponding thermodynamic values of selected species in reaction are shown in Table 2. Both high-spin and low-spin potential energy surfaces have been characterized in detail. The computations indicate that the stationary points of high-spin states are higher in energy than those of the low-spin states, and the whole reaction proceeds on the ground-states potential energy surfaces with a spin-conserving manner, so we mostly discuss the ground states route of low-spin. As shown in Figure 2 and Table 2, the first step of the reaction is the formation of precursor complex, HM^+-CH_4, which the computed binding energies for RuH^+CH_4 (a_1), RhH^+CH_4 (b_1), and PdH^+CH_4 (c_1) are 21.8, 22.2, and 19.7 kcal/mol, respectively. Thus, the methane is strongly bound in these complexes. Next, this encounter complexes HM^+-CH_4 proceed via a properly characterized, σ-metathesis-like transition structure $[M(H)(H)(CH_3)]^+$ from which the stable intermediates $(MCH_3^+)H_2$ are formed. Corresponding barriers are 7.2, 8.2, and 10.6 kcal/mol, respectively. We note in particular the features of the transition structure $[M(H)(H)(CH_3)]^+$ in which the migrating hydrogen atom H2 interacts with three centers simultaneously, that is, the carbon, ruthenium, and hydrogen

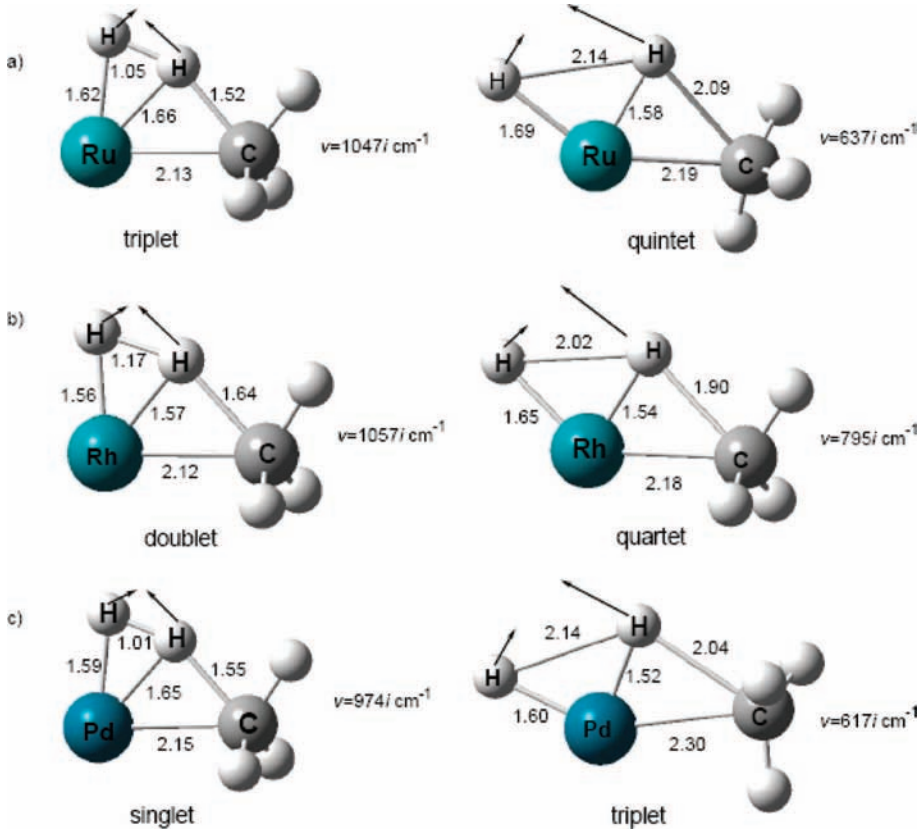

Figure 1. Structures of $MHHCH_3^+$ (M = Ru, Rh, and Pd) transition states species. Bond lengths are for the low-spin and high-spin species in angstroms. Arrows indicate the transition vectors. Imaginary frequencies of the vectors are shown at right.

H1 atoms. As required for an s-metathesis process, the atoms H1, H2, M, and C are coplanar (shown in scheme 1). Ultimately, the elimination of dihydrogen in the intermediates $(RuCH_3^+)H_2$ (a_3), $(RhCH_3^+)H_2$ (b_3), and $(PdCH_3^+)H_2$ (c_3) require energies of 11.4, 21.2, and 13.8 kcal/mol, respectively, yielding metal methyl ions $RuCH_3^+$ (A), $RhCH_3^+$ (B), and $PdCH_3^+$ (C). The overall hydrogenation reactions catalyzed by the cationic MH^+ have free energies of reaction $\Delta G°$ of −11.0, −1.2, and −5.2 kcal/mol.

The thing worthy to say is that the MCTS is related to the most important electronic process, which is responsible for the C−H bond dissociation of methane. The calculated activation energies $\Delta E^‡$ relative to the dissociation limit for RuH^+, RhH^+, and PdH^+ are −14.6, −14.0, and −9.1 kcal/mol, respectively. We expect from the negative values that methane should be effectively activated by RuH^+, RhH^+, and PdH^+. Speaking of the three complexes, the reaction activities gradually weaken from RuH^+ to PdH^+ with the values of $\Delta E^‡$ gradually increasing.

D. Comparison to MH^+ (M = Fe, Co, and Ni) and M^+ (M = Ru, Rh, Pd). The thermal reactions of MH^+ (M = Ru, Rh, Pd) and their first-row congeners with methane have many features in common; however, fundamental differences exist with regard to the details of the potential energy surfaces and thus to the actual reaction mechanisms. As already shown by Zhang and Bowers,[27] the Fe-, Co-, and Ni-mediated H/CH_3 ligand exchange constitutes a textbook example for the operation of "two-state reactivity"[39,40] because crossings between the high-spin and low-spin potential energy surfaces take place at both the entrance and the exit channels of reaction. Thereby, a pathway is opened up that bypasses an energetically rather unfavorable transition structure associated with a spin-conserving σ-metathesis process on the high-spin ground-state surface. In distinct contrast, the MH^+/CH_4 (M = Ru, Rh, Pd) couple can be fully explained without invoking a multistate pattern; instead, the whole reaction proceeds on the ground-states potential-energy surface in a spin-conserving manner. Spin inversion occurs in the reaction of MH^+ (M = Fe, Co, and Ni) and methane, so they can not be totally transformed into products of the ground states because of the transition probabilities; the reaction of MH^+ (M = Ru, Rh, and Pd) and methane does not exist electronic transition phenomenon, therefore the experimental yield is expected to relatively higher.

Another difference is energy barrier. The reaction energy barriers are measured to be 11.7, 1.9, and <0 kcal/mol relative to the separated reactants for Fe, Co, and Ni, respectively,[27] and the transition states are all located below the entrance channel for Ru, Rh, and Pd. It is possible that the energy barriers differences in the reactions processes may be related to bonding differences for the first-row vs second-row transition metal ions, and these differences can be obtained from an examination of the bond strengths and bonding atom orbitals used for the transition metal ion reactions. For the first-row metal hydrides, the ground states of the diatomic metal hydrides FeH^+, CoH^+, and NiH^+ indicate that the bonding in these molecules involves a metal orbital which is 85−90% s-like in character.[41] The bond dissociation energies for the first-row transition metals increase with decreasing promotion energy from the ground state to a state with an electronic configuration which is s^{1-n}, indicating a bond that involves a metal 4s orbital.[42] Because the first bond utilizes what is primarily a 4s orbital, formation of a second bond to Fe^+, Co^+, and Ni^+ involves primarily a metal 3d orbital.[41] The second bond is thus inherently weaker than the first due to the smaller size and poorer overlap of the 3d orbital relative to the 4s orbital. The description of the bonding to the second-row metal ions, however, is quite different. When bonding a hydrogen atom to the ground states of Ru^+, Rh^+,

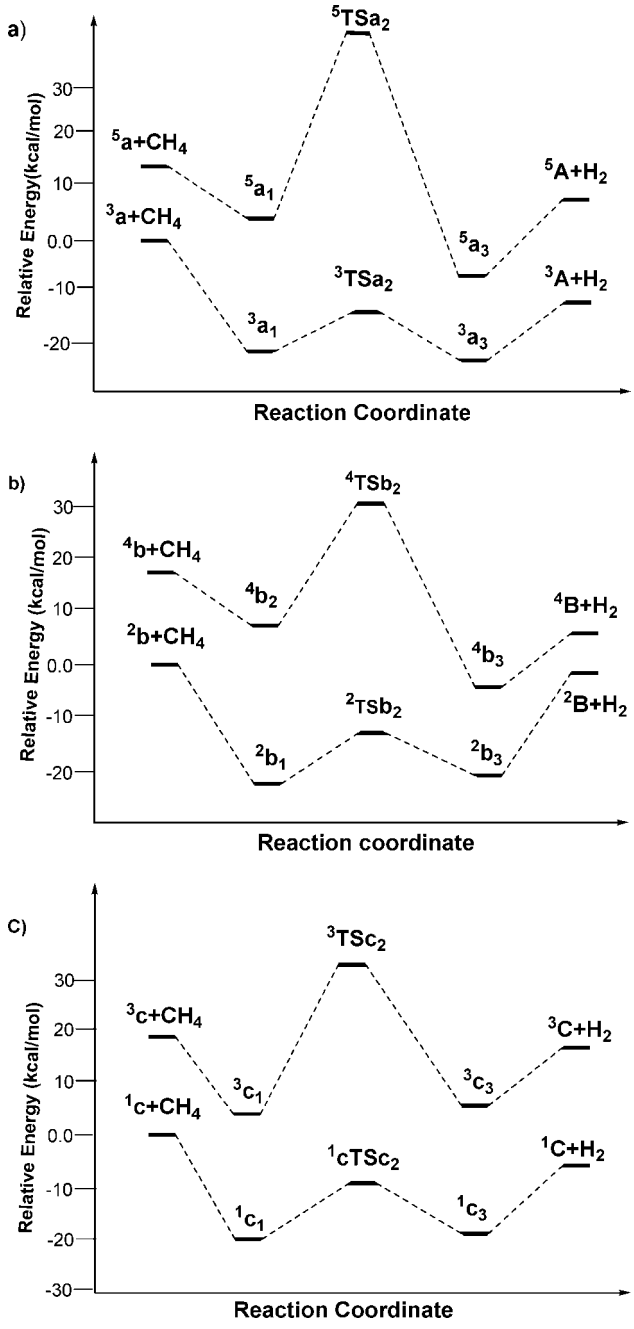

Figure 2. Reaction coordinate diagrams for the complexation and C−H bond activation reactions $MH^+ + CH_4 \rightarrow MCH_3^+ + H_2$. (a) M = Ru, (b) M = Rh, (c) M = Pd.

and Pd^+, which are all derived from d^n configurations, the metal orbital involved is predominantly d-like in character[37] because

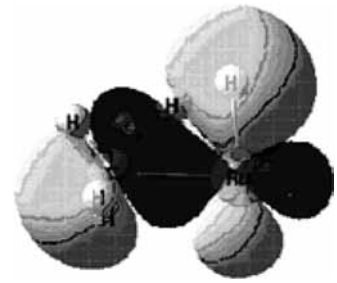

Figure 3. Molecular orbitals of the Ru^+HHCH_3 MCTS.

of the more similar size of the 5s and 4d orbitals in the second-row transition series. Thus, the second bond to Ru^+-H and $Rh-H^+$ might be expected to have the same inherent bond energy as the first bond. Furthermore, because less exchange energy is lost in forming the second bond to a d orbital, the second bond might actually be stronger than the first.[43] However, as indicated in Table 1, the first bond energy tends to be somewhat greater for the first-row metal ions than for the second (BDE: FeH^+, 53; CoH^+, 48; NiH^+, 39 kcal/mol).[44] Therefore, the sum of the first and second bond energies may be comparable for the metal ions of both rows. Note, however, that the orbitals used in forming these bonds are quite different for the metal ions of the two rows, and this may be responsible for the differences.

The methane activation by cations naked transition metal atoms has been studied previously.[45] The results demonstrate that no insertion minima are obtained for ruthenium and palladium in the geometry optimization procedure. For rhodium, the ground-state in the insertion product region is a triplet state, corresponding to a covalently bound d^7s^1 configuration and originating from the ^5F excited atomic state. (The quintet state of the rhodium atom forms two covalent bonds to the doublet hydrogen and the doublet methyl group, yielding a triplet state of the final product.) The $Rh^+ + CH_4 \rightarrow RhCH_2^+ + H_2$ reaction path also has previously been studied theoretically by Blomberg,[46] using B3LYP calculations with double-ζ plus polarization basis set, indicating that there is no barrier in excess of the endothermicity of the H_2 elimination reaction. However for RuH^+, RhH^+, and PdH^+, our theoretical studies predict that the reactions could occur efficiently by direct dehydrogenation mechanisms. The s electrons will be involved in the bonding between the metal and the hydrogen ligand and will therefore be removed from the part of the space where the methane molecule is approaching. This will lead to a decrease of the repulsion. As shown in Figure 3, in the four-centered transition states, there is one molecular orbital that is more critical than any of the others. This molecule orbital is a linear combination of a metal d_{xy} orbital, a hydride 1s orbital, and the sp^3-hybridized orbitals on methyl. This linear combination makes the bond of

TABLE 2: Calculated Thermodynamic Values (kcal/mol) at 298.15 K of the Reaction of MH^+ with CH_4 in Ground Electronic States

species	$\Delta E°$	$\Delta H°$	$\Delta G°$	species	$\Delta E°$	$\Delta H°$	$\Delta G°$
$^3a + CH_4$	0.0	0.0	0.0	$^1c + CH_4$	0.0	0.0	0.0
$^3a_1$	−21.8	−22.6	−15.7	$^1c_1$	−19.7	−20.7	−13.3
$^3TSa_2$	−14.6	−15.9	−7.8	$^1TSc_2$	−9.1	−10.3	−2.6
$^3a_3$	−22.5	−23.3	−16.1	$^1c_3$	−19.0	−19.9	−13.3
$^3A + H_2$	−11.1	−10.7	−11.0	$^1C + H_2$	−5.2	−4.9	−5.2
$^2b + CH_4$	0.0	0.0	0.0				
$^2b_1$	−22.2	−23.1	−16.2				
$^2TSb_2$	−14.0	−15.2	−7.4				
$^2b_3$	−20.0	−20.9	−13.7				
$^2B + H_2$	−1.2	−1.5	−1.2				

carbon−hydrogen broken and the bonds of metal−carbon, metal−hydrogen, and hydrogen−hydrogen formed. In the MCTS, the hydrogen ligand will simply remove some of the repulsive electrons on the metal and make the reactions barriers smaller.

As mentioned in the introduction, the reaction of methane dehydrogenation by PdH^+ has been reported by Schlangen and Schwarz.[27] The energy profile obtained by us is consistent both reactive mechanism and intercepted minima and transition state. A very big discrepancy concerns the value of the gap between the ground singlet and triplet excited states reported by Schwarz (>320 kJ/mol), which we calculated to be 81.5 kJ/mol. In order to get more accurate results, we calculated the spilt energy at the level of MP2 (98.3 kJ/mol) and CCSD (90.4 kJ/mol) with the above-mentioned basis set (ECP+6-31+G**). But the value (>320 kJ/mol) still could not be obtained. Therefore, Schlangen and Schwarz were likely to overestimate split energy of the PdH^+ largely.

IV. Conclusions

Theoretical calculations for the mechanism of methane catalyzed by ligated transition metal MH^+ (M = Ru, Rh, and Pd) have been carried out at the DFT (B3LYP) level, and some comparisons with their first-row congeners and their cations reaction with methane have been performed. The results illustrate that the activation of methane by MH^+ complexes is a concerted reaction via one transition states, which can competitively form metal methyl and hydrogen. Both high-spin and low-spin potential energy surfaces have been characterized in detail. The stationary points of high-spin states are higher in energy than that of the low-spin states, and the whole reaction proceeds on the ground-states potential energy surfaces with a spin-allowed manner. The activation energy barriers of reactions are located energetically below the entrance and exit channels, thus these complexes are good mediators for the activity of methane. The exothermicities of the reactions are close for Ru, Rh, and Pd at 11.1, 1.2, and 5.2 kcal/mol, respectively.

Acknowledgment. This research has been supported by the Natural Science Foundation of Gansu province (Grant No. 1071ORJZA114) and the Natural Science Foundation of Gansu province education office (Grant No.10801-10). These grants are gratefully acknowledged.

Supporting Information Available: Selected output from DFT calculations showing the Cartesian coordinates, sum of electronic and zero-point energies (au), and vibrational zero-point energies (au) for the reactants, transition states, and products reported in the manuscript are included here. The relativistic core potentials RECP in combination with their optimized basis set were used for Ru, Rh, and Pd in the present studies. The 6-31+G** basis set was used for C and H atoms. This material is available free of charge via the Internet at http://pubs.acs.org.

References and Notes

(1) Shilov, A. E.; Shul'pin, G. B. *Chem. Rev.* **1997**, *97*, 2879.
(2) Hall, C.; Perutz, R. N. *Chem. Rev.* **1996**, *96*, 3125.
(3) Arndsten, B. A.; Bergman, R. G.; Mobley, T. A.; Peterson, T. H. *Acc. Chem. Res.* **1995**, *28*, 154.
(4) Eller, K.; Schwarz, H. *Chem. Rev.* **1991**, *91*, 1121.
(5) Crabtree, R. H. *Chem. Rev.* **1985**, *85*, 245.
(6) (a) Reichert, E. L.; Thurau, G.; Weisshaar, J. C. *J. Chem. Phys.* **2002**, *117*, 653. (b) Reichert, E. L.; Weisshaar, J. C. *J. Phys. Chem. A* **2002**, *106*, 5563. (c) Yi, S. S.; Reichert, E. L.; Holthausen, M. C.; Koch, W.; Weisshaar, J C. *Chem.−Eur. J.* **2000**, *6*, 2232. (d) Porembski, M.; Weisshaar, J. C. *J. Phys. Chem. A* **2001**, *105*, 4851.
(7) (a) Loos, J.; SchrÖder, D.; Zummack, W.; Schwarz, H. *Int. J. Mass Spectrom.* **2002**, *217*, 169. (b) Barsch, S.; SchrÖder, D.; Schwarz, H. *Int. J. Mass Spectrom.* **2000**, *202*, 363. (c) Dieterle, M.; Harvey, J. N.; Heinemann, C.; Schwarz, J.; SchrÖder, D.; Schwarz, H. *Chem. Phys. Lett.* **1997**, *277*, 399.
(8) (a) Sicilia, E.; Russo, N. *J. Am. Chem. Soc.* **2002**, *124*, 1471. (b) Russo, N.; Sicilia, E. *J. Am. Chem. Soc.* **2001**, *123*, 2588.
(9) Walters, R. S.; Jaeger, T. D.; Duncan, M. A. *J. Phys. Chem. A* **2002**, *106*, 10482.
(10) (a) Zhang, X. G.; Liyanage, R.; Armentrout, P. B. *J. Am. Chem. Soc.* **2001**, *123*, 5563. (b) Armentrout, P. B.; Baer, T. *J. Phys. Chem.* **1996**, *100*, 12866. (c) Sievers, M. R.; Armentrout, P. B. *J. Chem. Phys.* **1995**, *102*, 754. (d) Chen, Y.; Armentrout, P. B. *J. Phys. Chem.* **1995**, *99*, 10775.
(11) (a) Kemper, P. R.; Weis, P.; Bowers, M. T. *Chem. Phys. Lett.* **1998**, *293*, 503. (b) Kemper, P. R.; Bushnell, J.; von Koppen, P. A. M.; Bowers, M. T. *J. Phys. Chem.* **1993**, *97*, 1810.
(12) (a) Achatz, U.; Beyer, M.; Joos, S.; Fox, B. S.; Niedner-Schatteburg, G.; Bondybey, V. E. *J. Phys. Chem. A* **1999**, *103*, 8200. (b) Albert, G.; Berg, C.; Beyer, M.; Achatz, U.; Joos, S.; Niedner-Schatteburg, G.; Bondybey, V. E. *Chem. Phys. Lett.* **1997**, *268*, 235.
(13) (a) Westerberg, J.; Blomberg, M. R. A. *J. Phys. Chem. A* **1998**, *102*, 7303. (b) Wittborn, A. M. C.; Costas, M.; Blomberg, M. R. A.; Siegbahn, P. E. M. *J. Chem. Phys.* **1997**, *107*, 4318.
(14) Blomberg, M. R. A.; Siegbahn, P. E. M.; Svensson, M. *J. Phys. Chem.* **1994**, *98*, 2062.
(15) (a) Jones, W. D.; Feher, F. J. *J. Am. Chem. Soc.* **1982**, *104*, 4240. (b) Sakakura, T.; Sodeyama, T.; Sasaki, K.; Wada, K.; Tanaka, M. *J. Am. Chem. Soc.* **1990**, *112*, 7221.
(16) (a) Zhang, Q.; Kemper, P. R.; Shin, S. K.; Bowers, M. T. *Int. J. Mass Spectrom.* **2001**, *204*, 281. (b) Zhang, Q.; Kemper, P. R.; Bowers, M. T. *Int. J. Mass Spectrom.* **2001**, *210*, 265.
(17) (a) Ekeberg, D.; Uggerud, E.; Lin, H. Y.; Sohlberg, K.; Chen, H. L.; Ridge, D. P. *Organometallics* **1999**, *18*, 40. (b) Chen, Q.; Chen, H. P.; Kais, S.; Freiser, B. S. *J. Am. Chem. Soc.* **1997**, *119*, 12879. (c) Chen, Y. M.; Clemmer, D. D.; Armentrout, P. B. *J. Am. Chem. Soc.* **1994**, *116*, 7815. (d) Armentrout, P. B. *Acc. Chem. Res.* **1995**, *28*, 430.
(18) (a) Carpenter, C. J.; van Koppen, P. A. M.; Bowers, M. T.; Perry, J. K. *J. Am. Chem. Soc.* **2000**, *122*, 392. (b) van Koppen, P. A. M.; Perry, J. K.; Kemper, P. R.; Bushnell, J. E.; Bowers, M. T. *Int. J. Mass Spectrom.* **1999**, *187*, 989.
(19) Eller, K.; Schwarz, H. *Chem. Rev.* **1991**, *91*, 1121.
(20) (a) Jacobson, D. B.; Freiser, B. S. *J. Am. Chem. Soc.* **1984**, *106*, 3891. (b) Jackson, T. C.; Jacobson, D. B.; Freiser, B. S. *J. Am. Chem. Soc.* **1984**, *106*, 1252.
(21) (a) Huang, S. K.; Allison, J. *Organometallics* **1983**, *2*, 833. (b) Freas, R. B.; Ridge, D. P. *J. Am. Chem. Soc.* **1980**, *102*, 7129.
(22) (a) Fiedler, A.; SchrÖder, D.; Shaik, S.; Schwarz, H. *J. Am. Chem. Soc.* **1994**, *116*, 10734. (b) Ryan, M. F.; Fiedler, A.; SchrÖder, D.; Schwarz, H. *Organometallics* **1994**, *13*, 4072.
(23) (a) Clemmer, D. E.; Aristov, N.; Armentrout, P. B. *J. Phys. Chem.* **1993**, *97*, 544. (b) Clemmer, D. E.; Chen, Y. M.; Khan, F. A.; Armentrout, P. B. *J. Phys. Chem.* **1994**, *98*, 6522.
(24) Ryan, M. F.; Fiedler, A.; SchrÖder, D.; Schwarz, H. *J. Am. Chem. Soc.* **1995**, *117*, 2033.
(25) SchrÖder, D.; Holthausen, M. C.; Schwarz, H. *J. Phys. Chem. B* **2004**, *108*, 14407.
(26) Zhang, Q.; Bowers, M. T. *J. Phys. Chem. A* **2004**, *108*, 9755.
(27) Schlangen, M.; Schwarz, H. *Angew. Chem., Int. Ed.* **2007**, *46*, 5614.
(28) Becke, A. D. *J. Chem. Phys.* **1993**, *98*, 5648.
(29) Becke, A. D. *Phys. Rev. A* **1988**, *38*, 3098.
(30) Lee, C.; Yang, W.; Parr, R. G. *Phys. Rev. B* **1988**, *37*, 785.
(31) Gonzalez, C.; Schlegel, H. B. *J. Chem. Phys.* **1989**, *90*, 2154.
(32) Glukhovtse, M. N.; Pross, A.; McGrath, M. P.; Radom, L. *J. Chem. Phys.* **1995**, *103*, 1878.
(33) Andrae, D.; Haeussermann, U.; Dolg, M.; Stoll, H. *Theor. Chim. Acta.* **1990**, *77*, 123.
(34) Dolg, M.; Stoll, H.; Savin, A.; Preuss, H. *Theor. Chim. Acta.* **1989**, *75*, 173.
(35) Dolg, M.; Stoll, H.; Preuss, H. *Theor. Chim. Acta.* **1993**, *85*, 441.
(36) Frisch, M. J.; Trucks, G. W.; Schlegel, H. B.; Scuseria, G. E.; Robb, M. A.; Cheeseman, J. R.; Zakrzewski, V. G.; Montgomery, J. A., Jr.; Stratmann, R. E.; Burant, J. C.; Dapprich, S.; Millam, J. M.; Daniels, A. D.; Kudin, K. N.; Strain, M. C.; Farkas, O.; Tomasi, J.; Barone, V.; Cossi, M.; Cammi, R.; Mennucci, B.; Pomelli, C.; Adamo, C.; Clifford, S.; Ochterski, J.; Petersson, G. A.; Ayala, P. Y.; Cui, Q.; Morokuma, K.; Malick, D. K.; Rabuck, A. D.; Raghavachari, K.; Foresman, J. B.; Cioslowski, J.; Ortiz, J. V.; Stefanov, B. B.; Liu, G.; Liashenko, A.; Piskorz, P.; Komaromi, I.; Gomperts, R.; Martin, R. L.; Fox, D. J.; Keith, T.; Al-Laham, M. A.; Peng, C. Y.; Nanayakkara, A.; Gonzalez, C.; Challacombe, M.; Gill, P. M. W.;

Johnson, B. G.; Chen, W.; Wong, M. W.; Andres, J. L.; Head-Gordon, M.; Replogle, E. S.; Pople, J. A. *Gaussian 98*; Gaussian, Inc.: Pittsburgh, PA, 1998.

(37) Schilling, J. B.; Goddard, W. A.; Beauchamp, J. L. *J. Am. Chem. Soc.* **1987**, *109*, 5565.

(38) Mandich, M. L.; Halle, L. F.; Beauchamp, J. L. *J. Am. Chem. Soc.* **1984**, *l06*, 4403.

(39) Schwarz, H. *Int. J. Mass Spectrom.* **2004**, *237*, 75.

(40) Rivalta, I.; Russo, N.; Sicilia, E. *J. Comput. Chem.* **2006**, *27*, 174.

(41) Schilling, J. B.; Goddard, W. A.; Beauchamp, J. L. *J. Am. Chem. Soc.* **1986**, *108*, 582.

(42) Armentrout, P. B.; Halle, L. F.; Beauchamp, J. L. *J. Am. Chem. Soc.* **1981**, *103*, 6501.

(43) Mandich, M. L.; Halle, L. F.; Beauchamp, J. L. *J. Am. Chem. Soc.* **1984**, *106*, 4403.

(44) Halle, L. F.; Armentrout, P. B.; Beauchamp, J. L. *Organometallics.* **1982**, *1*, 963.

(45) Blomberg, M. R. A.; Siegbahn, P. E. M.; Svensson, M. *J. Phys. Chem.* **1994**, *98*, 2062.

(46) Westerberg, J.; Blomberg, M. R. A. *J. Phys. Chem.* **1998**, *102*, 7303.

JP808830C